ALIEN EARTHS

Which Nearby Planetary Systems Are Likely to
Host Habitable Planets and Life?

MONTHLY NEWSLETTER

March 2026

Alien Earths is part of NASA's Nexus for Exoplanetary System Science program, which carries out coordinated research toward the goal of searching for and determining the frequency of habitable extrasolar planets with atmospheric biosignatures in the Solar neighborhood.

Our interdisciplinary teams include astrophysicists, planetary scientists, cosmochemists, material scientists, chemists, biologists, and physicists.

The Principal Investigator of Alien Earths is Daniel Apai (University of Arizona). The projects' lead institutions are The University of Arizona's Steward Observatory and Lunar and Planetary Laboratory.

For a complete list of publications, please visit the **AE Library** on the SAO/NASA Astrophysics Data System.

Recent Publications

Helium Escape in Context: Comparative Signatures of Four Close-in Exoplanets

Older Ages for 23 Pre-main Sequence Stars in Upper Scorpius Using Dynamical-mass-constrained Stellar Evolutionary Models

Molecular Hydrogen Controls the Temperatures of Flares on TRAPPIST-1

Forecasting Catastrophe: Constraints on the Fomalhaut Main Belt Planetesimal Population from Observed Collisional Remnants

The Radius Cliff is a Waterfall: Explaining Sub-Neptune Exoplanets with Steam Worlds

Gaps and Rings: A Near-Universal Trait of Extended Protoplanetary Discs

Not Earth-like yet Temperate? More Generic Climate Feedback Configurations Still Allow Temperate Climates in Habitable Zone Exo-Earth Candidates

The JWST Cool Star Spectral Library was selected for General Observer time

Helium Escape in Context: Comparative Signatures of Four Close-in Exoplanets

Anna Ruth Taylor, Tommi T. Koskinen, Chenliang Huang (黄辰亮), Anthony Arfaux, and Panayotis Lavvas

The Astrophysical Journal, Volume 999, Number 2

Observations of escaping atmospheres on close-in exoplanets show a wide range in the strength and morphology of He I 10830 Å and H I absorption. Scaling relations attempt to link the He I signal to X-ray and UV irradiation, mass loss, and bulk planetary parameters. We test these relations with a comparative analysis of HD209458b, HD189733b, HD149026b, and GJ1214b using a 1D hydrodynamic, multispecies, full-atmosphere escape model. For the benchmark HD209458b, our previously validated solution reproduces the observed He I and Hα transit depths without imposing composition constraints. HD189733b exhibits comparable He I depths, but the broadest reported profiles require ~12 km s^{-1} of additional nonthermal broadening, whereas more recent measurements are narrower, consistent with our predictions. For HD149026b, despite similar system properties, our model shows that higher gravity suppresses escape and enhances diffusive separation, depleting helium at high altitudes and yielding extremely weak He I absorption. For the sub-Neptune GJ1214b, H/He-only models overestimate He I absorption; including H_2 and its ions (H, H, HeH^+) lowers the escape rate and modifies the ion/electron balance, reducing the metastable helium densities. Compared against scaling relations, HD189733b observations and our HD149026b prediction fall below the trend, whereas some observations of HD209458b and GJ1214b are consistent; however, the observed transit depths are variable. Across all targets, we find diffusive separation of helium and hydrogen, which may explain why subsolar He/H ratios are often required in simplified models. We conclude that interpreting He I and Hα absorption requires first-principles models that include self-consistent temperature and velocity profiles, multispecies transport, and molecular chemistry.

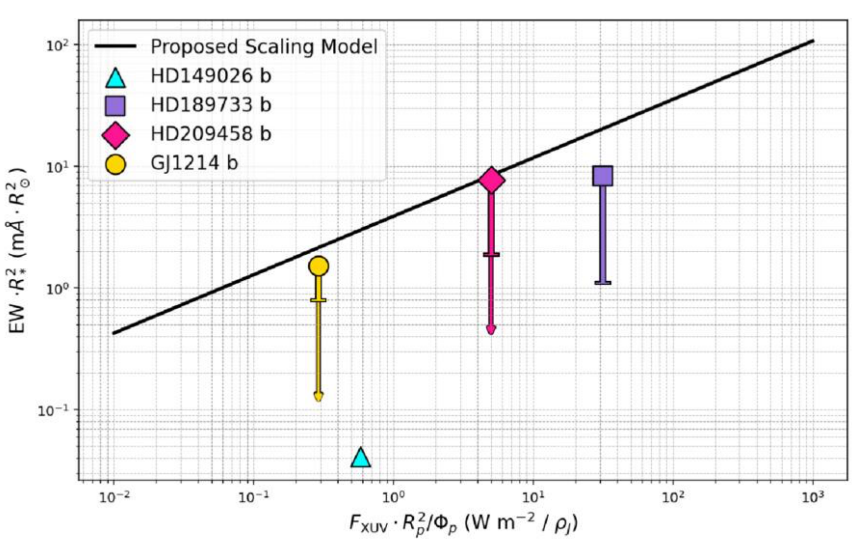

Figure 2. Recreation of the proposed scaling relation from J. Sanz-Forcada et al. (2025). Symbols indicate results for the four planets in this study. The points for HD209458b, HD189733b, and GJ1214b are based on observations, while the point for HD149026b is based on our model prediction. Lower error bar limits for GJ1214b and HD209458b are given by upper limits in A. Masson et al. (2024), and the lower limit for HD189733b is given by J. Orell-Miquel et al. (2025). The solid black line shows the predicted scaling of EW with $F_{XUV,He}$. Note that for the x-axis, we use the $F_{XUV,He}$ flux given in the last row of Table 1.

Older Ages for 23 Pre-main Sequence Stars in Upper Scorpius Using Dynamical-mass-constrained Stellar Evolutionary Models

A.P. M. Towner, J. A. Eisner, P. D. Sheehan, L. A. Hillenbrand, and Y.-L. Wu

The Astrophysical Journal, Volume 999, Number 1

We present revised stellar ages for 23 pre-main-sequence (PMS) K- and M-type stars in the Upper Scorpius (Upper Sco) star-forming region, derived using stellar dynamical masses to constrain isochronal ages from five PMS stellar evolutionary models. We find that mass-constrained stellar ages for all model sets are more consistent with the older, ~8–11 Myr age for Upper Sco derived using earlier-type stars. Additionally, applying the independent mass constraint to isochronal ages tends to (1) increase stellar ages for most model sets, and (2) decrease age scatter for individual sources between model sets. Models that account for global magnetic fields consistently provide the best match to our observations: they change comparatively little when the mass constraint is applied, and produce 9–10 Myr ages under both unconstrained and mass-constrained conditions. Most standard (nonmagnetic) models produce younger ages (3–5 Myr) when unconstrained, but older ages (6–9 Myr) when constrained by dynamical mass. Our results are consistent with recent literature findings that suggest median disk lifetimes may be ≳2× longer than previously thought.

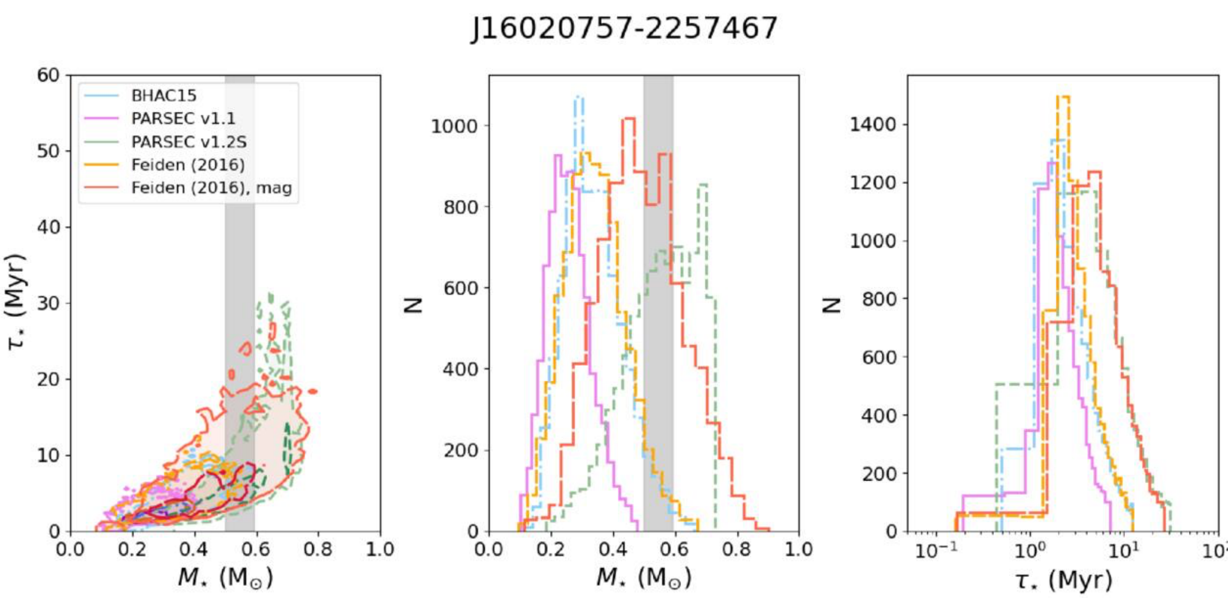

Figure 1. Isochronal masses and ages for example source J16020757−2257467. Left: contour plots of isochronal age (τ_{all}) vs. isochronal mass (M_{iso}) for all five model sets considered in this work. The vertical gray bar denotes the disk-derived dynamical mass, including uncertainties. The portions of each set of contours that overlap the gray bar are what comprise our mass-constrained age (τ_{dyn}) for a given source. Center: histograms of the distribution of isochronal mass for each of the five model sets. The gray bar again denotes the derived dynamical mass, including uncertainties. Right: histograms of the distribution of unconstrained isochronal age (τ_{all}) for each model set. Note the logarithmic scale on the *x*-axis. The mass-constrained ages for this source (τ_{dyn}) are as follows: 11 ± 8 Myr (BHAC15), 8 ± 5 Myr (PARSEC v1.1), 6 ± 4 Myr (PARSEC v1.2S), 10 ± 5 Myr (nonmagnetic G. A. Feiden 2016), and 9 ± 5 Myr (magnetic G. A. Feiden 20

Molecular Hydrogen Controls the Temperatures of Flares on TRAPPIST-1

A.I. Shaprio, N. Kostogryz, S. Seager, V. Witzke, J de Wit, V. Vasilyev, Astrid M Veronig, Cameron Robert, Peter Hardi, S.K. Solanki

The Astrophysical Journal, Volume 998, Number 1

Early JWST observations of TRAPPIST-1 have revealed an unexpected puzzle: energetic white-light flares ($E > 10^{30}$ erg) reach temperatures of only ~3500–4000 K, nearly 3 times cooler than typical solar flares, which peak around 9000–10,000 K. Here we explain this difference by identifying the physical mechanism that regulates flare temperatures on late M dwarfs. The key factor is that in the cool, dense atmosphere of TRAPPIST-1, magnetic heating is strongly moderated by the dissociation of molecular hydrogen (H_2) into atomic hydrogen. This "H_2 dissociation thermostat" acts as an efficient energy sink, preventing flare regions from heating above ~4000 K. Our chemical equilibrium and heat capacity calculations show that this effect depends sensitively on stellar atmospheric pressure and the local abundance of H_2. In hotter stars, from early M dwarfs to solar-type stars, the scarcity of molecular hydrogen renders this mechanism ineffective; instead, atomic hydrogen ionization limits flare temperatures near ~9000 K.

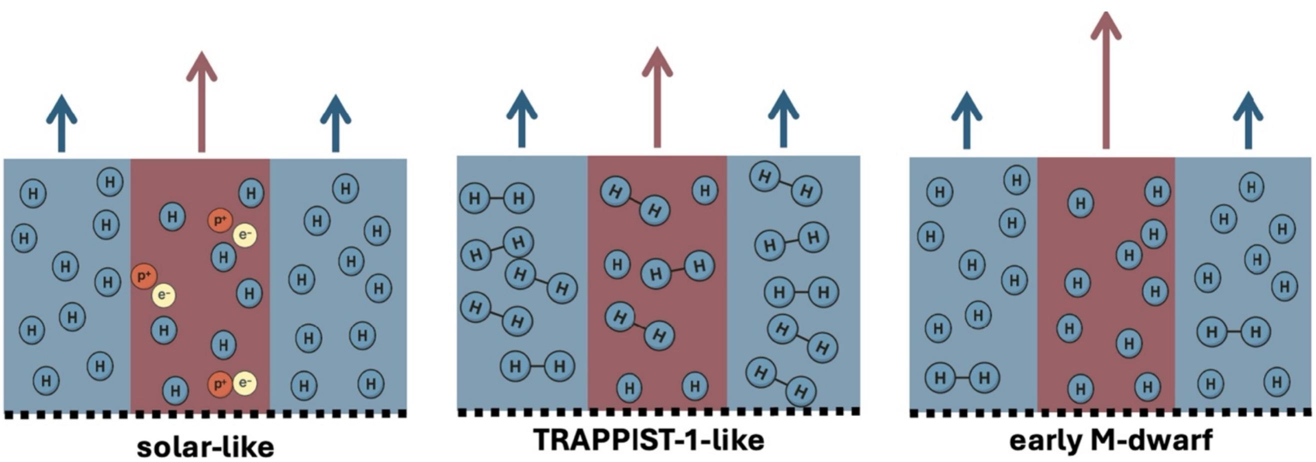

Figure 1. Illustration of flare heating in three types of stars. The dashed line marks the stellar surface; blue areas show the quiet atmosphere, and red areas show regions heated during a white-light flare. Vertical arrows indicate the radiative output, with length proportional to intensity. In solar-like stars (left), heating is regulated by hydrogen ionization, which limits the temperatures of white-light flares to ~9000 K. In late M dwarfs like TRAPPIST-1 (middle), molecular hydrogen dissociation acts as a thermostat, capping the temperatures of white-light flares near ~3500–4000 K. In early M dwarfs (right), insufficient concentration of H_2 means the dissociation thermostat is ineffective, allowing higher white-light flare temperatures.

Forecasting Catastrophe: Constraints on the Fomalhaut Main Belt Planetesimal Population from Observed Collisional Remnants

Arin M. Avsar, Kevin Wagner, Dániel Apai, Christopher Stark, Isabel Rebollido

Astro-ph: arXiv: 2603.07376

Catastrophic planetesimal disruptions offer a unique opportunity to study and characterize large planetesimal populations in exoplanetary systems that are not currently detectable by modern observatories. The unexpected discovery of a second collision event in the Fomalhaut system raises important questions about the planetesimal population and dynamical state inside the Fomalhaut main belt that led to two collisions in 20 years. We present a statistical model developed and applied to the archetypal Fomalhaut system to provide new constraints on the bulk properties of the planetesimals in Fomalhaut's main belt. Utilizing the constraints provided by the spatially resolved Fomalhaut cs1 and cs2 collision events, we retrieve the belt parameters that best reproduce the observed collision rate while remaining consistent with the system's age and dust mass. Our best-fit model suggests a total main belt mass of 200-360 km and a maximum planetesimal radius of km. We estimate a catastrophic collision rate of collision events per year for planetesimals with radii 100 km in the region interior to the main belt. Our findings show that further observable collisions are likely, motivating continued monitoring of Fomalhaut and other nearby debris disks.

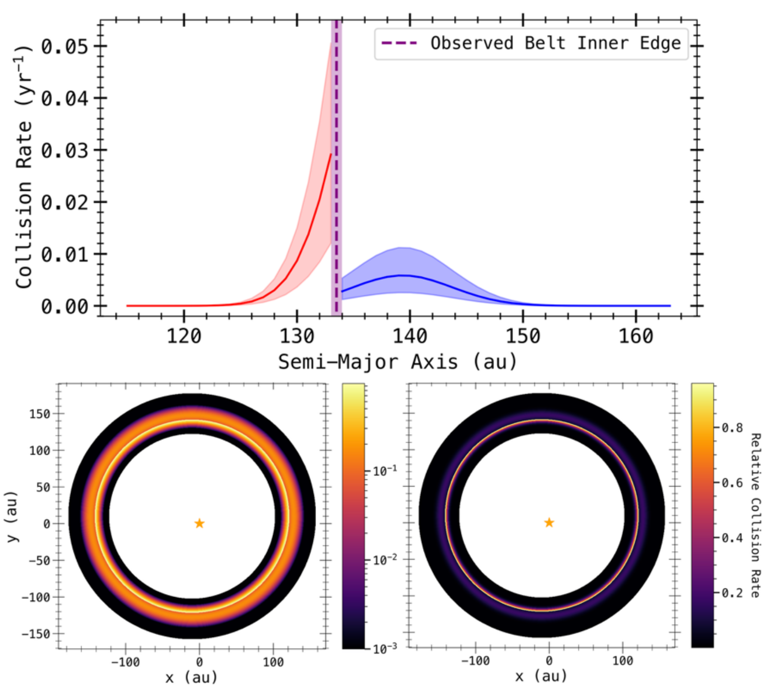

Figure 6. Top: The catastrophic collision rate for target planetesimals ≥ 100 km in radius as a function of belt semi-major axis. The blue region indicates the observed Fomalhaut main belt, and the red region indicates the region where Fomalhaut cs1 and cs2 originated, which is within observed belt inner edge. We find the highest collision rate at the observed inner edge of the Fomalhaut main belt. The shaded regions indicate the 16th and 84th percentiles of the posterior distribution. We find a very low collision rate interior to 125 au due to the low surface density of planetesimals in that region. We find a non-negligible collision rate in the observed main belt region. Bottom: Belt schematics outlining the relative collision rate for target planetesimals ≥ 100 km in radius. The two images plot the same data, with the left on a logarithmic scale and the right on a linear scale. The brightest band in both images is the location of observed belt inner edge and the location where the collision rate peaks. This is coincident with the discovery location of the most recent collision, Fomalhaut cs2.

The Radius Cliff is a Waterfall: Explaining Sub-Neptune Exoplanets with Steam Worlds

Aritra Chakrabarty, Gijs D. Mulders, Artyom Aguichine, and Natalie Batalha

The Astrophysical Journal, Volume 999, Number 2

The demographics of Kepler planets provide a key testbed for models of planet formation and evolution, particularly for explaining the radius valley separating super-Earths and sub-Neptunes. A primordial interpretation based on differences in bulk densities—where rocky and water-rich planets form via migration pathways—offers an alternative to atmospheric loss scenarios. Updated interior structure models of water worlds with adiabatic steam atmospheres reproduce the observed valley near ~2 $R_\oplus$ more accurately. Furthermore, migration models from our Genesis library suggest that these formation pathways can also account for the distinct period distributions of super-Earths and sub-Neptunes, as well as the emergence of the hot Neptune desert. Motivated by this, we develop a Bayesian hierarchical mixture model for close-in Kepler planets (P < 100 days), combining rocky planets and water worlds without H/He envelopes. The inferred mass distributions of rocky and water-rich planets peak at ~2.6 and ~7 $M_\oplus$, respectively, with the water mass fraction of water worlds peaking at ~41%. Water worlds provide a good representation of the Kepler sub-Neptune population, with the radius cliff emerging as a "waterfall"—a sharp decline in their occurrence. However, our mass–radius analysis shows that water worlds alone cannot explain planets with $R \gtrsim 3\ R_\oplus$, implying that at least ~20% of sub-Neptunes in the sample are enriched in H/He gas.

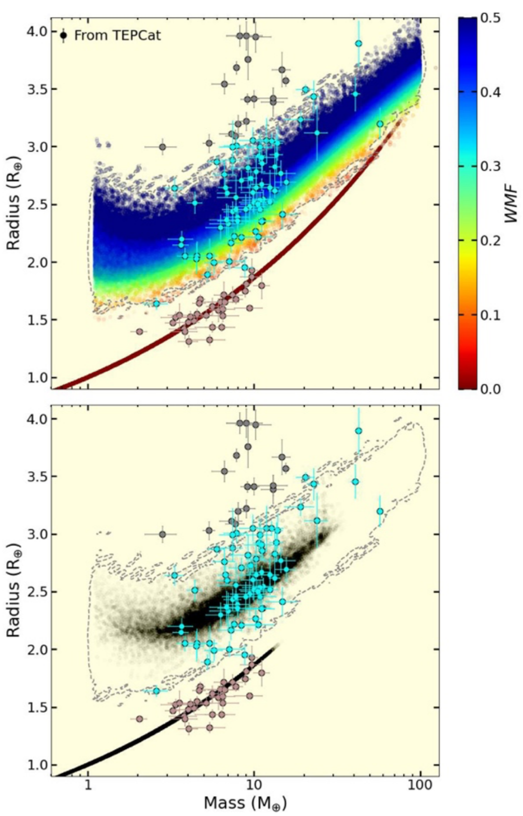

Figure 7. Mass–radius distribution of planets from Model I compared with the observed planets around G-type host stars from the TEPCat catalog (J. Southworth 2011). Top: weighted mass–radius distribution of simulated rocky planets and water worlds, shown with a color map of WMF. Bottom: the same weighted distribution shown without the WMF color map, with weight contours highlighted to illustrate regions of higher model likelihood and observational completeness. The model broadly agrees with the observed distribution for planets smaller than ~3 $R_\oplus$ in regions of high weights but fails to explain planets larger than ~3 $R_\oplus$, suggesting the presence of a H/He-rich population, comprising ~15% of the full TEPCat sample and ~20% of the TEPCat sub-Neptunes.

Gaps and Rings: A Near-Universal Trait of Extended Protoplanetary Discs

Quincy Bosschaart, Osmar M. Guerra-Alvarado, Nienke van der Marel, Gijs D. Mulders

Astro-ph: arXiv: 2602.12906

Substructures such as rings, gaps, and cavities are commonly observed in protoplanetary discs and are thought to play a key role in dust evolution and planet formation. However, a fraction of the extended discs (68% dust radii > 30 AU) in nearby star-forming regions remain unresolved, leaving their substructure content uncertain and thereby limiting our understanding of dust evolution and the initial conditions for planet formation across the full disc population. We aim to investigate the presence of substructures in previously unresolved, extended discs to assess whether all extended protoplanetary discs in the Solar neighbourhood exhibit substructures. We present new high-resolution (~0.12") ALMA Band 6 continuum observations at 1.33 mm of 26 previously unresolved, extended discs within 200 pc, completing the high-resolution sample of extended discs in Taurus, Ophiuchus, Chamaeleon, Lupus, Upper Scorpius, Upper Centaurus-Lupus and Lower Centaurus-Crux. We analyse radial intensity profiles using Frankenstein and Galario to detect substructures. Seventeen discs show clear substructures, while nine appear compact and structureless, smooth or ambiguous due to inclination or possible binarity/late-stage infall. We detect ^{12}CO J=2-1 emission in 15 discs, with extended emission in four. Combined with literature data, our complete sample of 730 protoplanetary discs reveals that nearly all extended discs exhibit substructures, ~91% detected in the full sample, and up to ~98% when correcting for high-inclination systems where substructures may be hidden. Substructures are a near-universal feature of extended protoplanetary discs. They are more commonly detected in larger, massive discs and around higher-mass stars, and structured discs retain their dust mass over time. This supports the scenario in which dust traps, possibly induced by giant planets, shape disc morphologies.

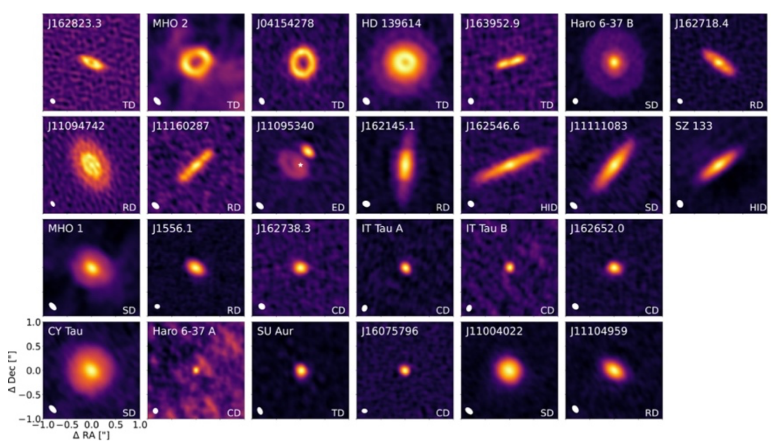

Fig. 1: Gallery of the 1.3 mm cleaned continuum emission images for the full sample. All images were cleaned using a Briggs weighting scheme with a robust value of +0.5, except for SSTc2d J163952.9-241931 and SSTc2d J162718.4-243915 (robust = 0.0), and SSTc2d J162823.3-242241 and 2MASS J11094742-7726290 (robust = -0.5). RA and Dec offsets from the disc centre are shown in arcseconds on the x- and y-axes, respectively. To emphasise the weak outer emission of a few discs, an asinh scaling function was applied. Each panel spans 2.0" × 2.0", with white ellipses in the lower left corner indicating the beam sizes. The colour scale represents the intensity in Jy/beam. The final disc classifications are marked in the lower right corner: TD (transition disc), RD (ring disc), SD (shoulder disc), HID (highly-inclined disc), CD (compact disc), ED (extended disc). For discs with names starting with SSTc2d, 2MASS, or RX, the names in the upper left corners are abbreviated to the first part after "J" (e.g., SSTc2d J162823.3-242241 is labelled as J162823.3). The white star in 2MASS J11095340-7634255 marks the current position of the central star.

Not Earth-like yet Temperate? More Generic Climate Feedback Configurations Still Allow Temperate Climates in Habitable Zone Exo-Earth Candidates

Chaucer Langbert and Dániel Apai

The Planetary Science Journal, Volume 7, Number 3

Earth's climate is influenced by over a dozen types of feedback, but only three dominate its long-term climate behavior. Models of the exoplanet habitable zone (HZ) assume that this is similar for other Earth-like planets. We used dynamical simulations to study Earth-like planets with a fourth (potentially strong) generalized climate feedback. Across over 20,000 climate simulations, we find that the addition of the fourth feedback produces novel behaviors, including runaway and chaotic climate trajectories, that are more diverse than one would expect based on Earth's climate configuration. Nonnegligible fourth feedbacks—if negative—would not lessen the probability of planets with temperate climates. However, a positive fourth feedback decreases the fraction of exo-Earth candidates that are long-term habitable. Therefore, strong fourth feedbacks will alter (and mostly shrink) the boundaries of the classical HZ. When combined with occurrence rates of Earth-sized planets around Sun-like stars, our results imply that the fraction of stars hosting rocky planets with temperate climates may be substantially lower than classical estimates under Earth-like climate assumptions. Our results are subject to the validity of the model assumptions and not intended to represent conclusive predictions about exoplanet populations but rather to demonstrate the potential climate diversity that emerges from non-Earth-like model configurations. Our conclusions provide context on sample sizes and science questions for next-generation exoplanet surveys.

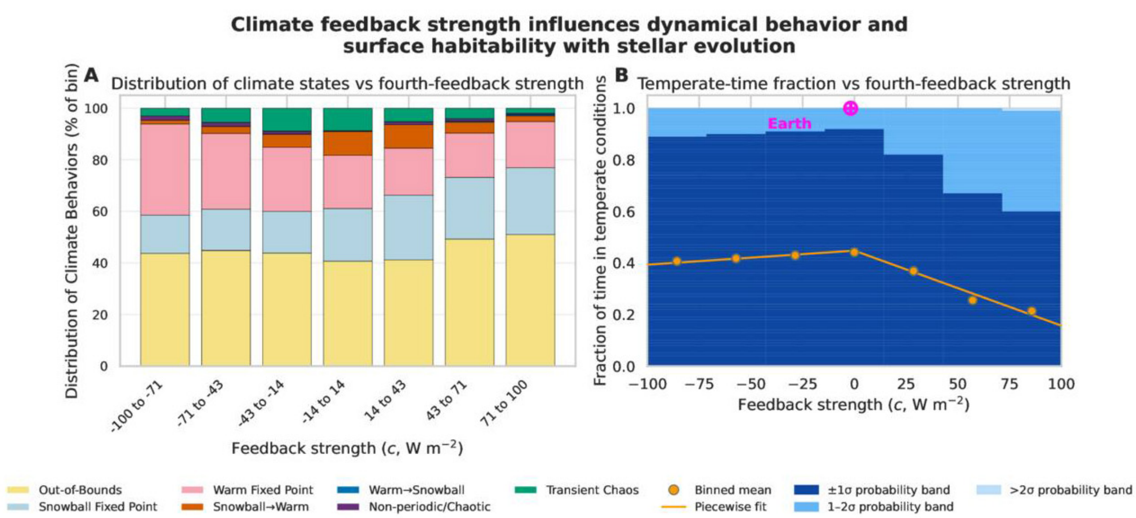

Figure 8. Climate behavior and time spent in habitable surface conditions as a function of the fourth feedback strength c (W m^{-2}), now incorporating stellar evolution. (A) Relative occurrence of climate behaviors binned by fourth-feedback strength c. Stable fixed points dominate across most bins, but transitions (snowball → warm, warm → snowball) and rare chaotic states appear near intermediate c. Out-of-bounds trajectories (gray) are more common at large $|c|$. (B) Fraction of time spent in temperate conditions as a function of c. Orange circles mark binned means, with a linear fit in orange and probability bands ($\pm1\sigma$, 1σ–2σ, $>2\sigma$) in blue shading. Earth's present-day location is marked in magenta. Strong negative feedbacks increase the likelihood of stable climates, whereas strong positive feedbacks greatly decrease the fraction of exo-Earth candidates that are long-term habitable.

The JWST Cool Star Spectral Library was selected for General Observer time with the requested allocation of 79.7 hours

(1 of 254 approved proposals out of 2,855 submitted)

Proposal Team:
CoI Prof. Daniel Apai University of Arizona USA/AZ
CoI Dr. Luigi R. Bedin INAF - Osservatorio Astronomico di Padova ITA
PI Dr. Mark S. Giampapa University of Arizona USA/AZ
CoI Dr. Kevin K. Hardegree-Ullman California Institute of Technology USA/CA
CoI Dr. Aishwarya Iyer NASA Goddard Space Flight Center USA/MD
CoI Dr. Chia-Lung Lin University of Arizona USA/AZ
CoI Dr. Benjamin Rackham Massachusetts Institute of Technology USA/MA
CoI Dr. Alexander I. Shapiro University of Graz, Austria

Limited fidelity in stellar models poses a bottleneck in multiple fields of astrophysics, including correcting exoplanet transmission spectra for host star heterogeneity ("stellar contamination"). Accurate corrections for magnetically active stellar surface regions require either refined model precision or empirical solutions. We propose establishing a JWST Spectral Library for Cool Stars, providing high-precision, flux-calibrated spectra critical for validating and refining current stellar model atmospheres. This library will benchmark next generation models and offer empirical spectra for accurate transmission spectrum corrections. Featuring high-resolution NIRSpec spectra of 43 carefully selected magnetically quiescent stars (3200 K–5000 K) across a broad metallicity range, it will encompass ~90% of known transiting exoplanet hosts amenable to JWST transmission spectroscopy. The project will enhance atmospheric characterizations of rocky planets and provide an immediate, valuable community resource for modeling cool stellar atmospheres, thus supporting JWST's mission and serving as a legacy asset.

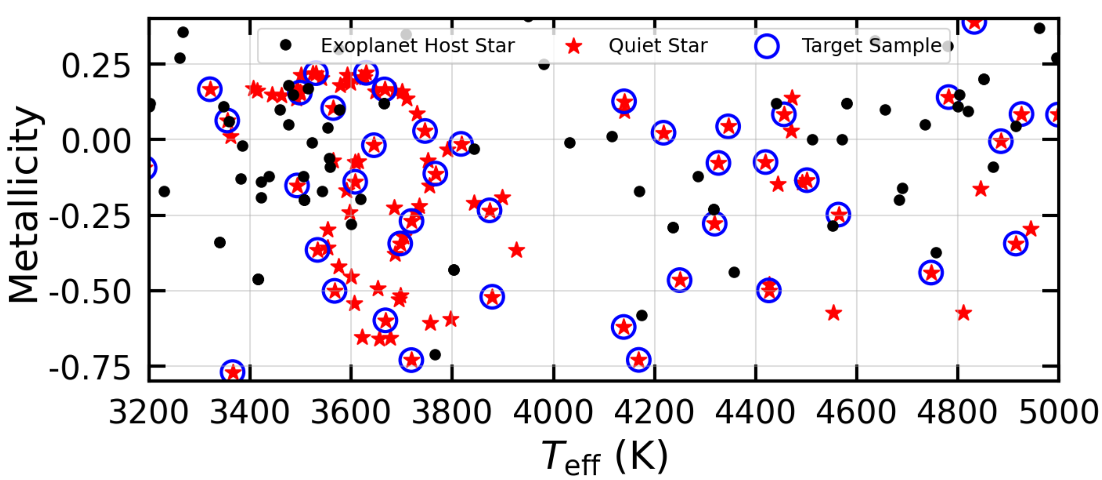

Overlap of quiescent K and M dwarfs (red stars) with transiting exoplanet hosts (black dots) in stellar Teff and metallicity space. The range of targets selected for this proposal (blue circled red stars) allows for broad expansion and testing of model atmospheres in this parameter space.